JOURNAL OF AIRCRAFT
Vol. 45, No. 2, March–April 2008

Personalized Ventilation for Commercial Aircraft Cabins

N. P. Gao and J. L. Niu*
Hong Kong Polytechnic University, Hung Hom, Kowloon, Hong Kong, People's Republic of China

DOI: 10.2514/1.30272

Complaints about cabin air quality and persistent reports of spreading infections on commercial flights indicate that continued investigations of cabin air systems and effective measures to improve cabin air quality are required. This study used a computational fluid dynamics technique to investigate the dispersion characteristics of sneezed/coughed particles by both the Eulerian and Lagrangian methods. These particles can be transported to a location more than three rows in front of the sneezing person, and less than 20% of the particles were exhausted, whereas the remainders are deposited owing to the high surface-to-volume ratio. Personalized ventilation, through the distribution of fresh air directly in the breathing zone, was able to shield up to 60% of air pollutants in a passenger's inhalation.

Nomenclature

C	=	particle concentration, g/m^3
C_C	=	Cunningham correction factor
d_p	=	particle diameter, μm
$\boldsymbol{F}_{\text{addi}}$	=	other additional force per unit mass, N
$\boldsymbol{F}_{\text{drag}}$	=	drag force per unit mass, N
$\boldsymbol{F}_{\text{grav}}$	=	gravity force per unit mass, N
$\boldsymbol{g}$	=	gravitational acceleration, m/s^2
S_C	=	particle source term, g/sm^3
t	=	time
$\boldsymbol{U}$	=	velocity vector, m/s
$\boldsymbol{u}_p$	=	particle velocity, m/s
$\boldsymbol{V}_S$	=	gravitational settling velocity calculated from Stokes's law, m/s
λ	=	molecular mean free length, μm
μ	=	molecular viscosity of the air, g/ms
μ_{eff}	=	turbulent effective viscosity, g/ms
ρ	=	air density, kg/m^3
ρ_p	=	particle material density, kg/m^3
σ_c	=	nondimensional number 1.0

I. Introduction

A COMMERCIAL aircraft cabin is suspected to be a high-risk environment for the transmission of infectious disease because of crowded space, limited ventilation, and prolonged exposure time. Since 1946, a number of outbreaks of serious infectious diseases aboard commercial airlines have been reported, such as influenza, tuberculosis, and severe acute respiratory syndrome (SARS) [1,2]. The risk of virus transmission during commercial air travels and the potential of commercial aircraft serving as vehicles of pandemics have recently gained more interest, especially after the SARS outbreaks in 2003. However, accurate epidemiological studies and public health surveys of disease transmission on aircraft are difficult, almost impossible, to perform. There are difficulties with the detection of infectious cases, providing the source of infection, and generalizing the results of one outbreak to other circumstances. The infected passengers might arrive at their destination before the end of the incubation period and might therefore spread diseases before symptoms develop [3]. This is, at least partly, the reason why virus transmission mechanisms from person to person in cabin environments are not exactly known.

In this study we used a computational fluid dynamics (CFD) technique [4] to study the dispersion of passenger-generated virus-containing aerosols under the current cabin air distribution design and also with the application of a personalized ventilation (PV) nozzle integrated with a seat (Fig. 1). The fresh air supply nozzle is adjustable, and should the occupant need to exercise some movement, the ventilation nozzle can be conveniently positioned aside, still functioning as a normal air supply outlet. This ventilation system is especially applicable to a long-distance commercial flight during which the occupant is seated for a prolonged period. The performance of this ventilation seat, regarding the user's exposure reduction to various pollutants, was simulated.

II. Methods

To obtain insight into the general airflow pattern, a three-dimensional CFD model of a five-row section of a Boeing 767-300 cabin was constructed (Fig. 2). The length in the X, Y, and Z directions was 4.7, 4.324, and 2.098 m, respectively. The aisle width was 0.5 m. Two different air distribution methods were compared. One was the existing mixing ventilation (MV) in which the air was replenished by the two ceiling inlets at a rate of 10 l/s/person. The other used the ventilation seat to serve the air to the breathing zones at 2.5 l/s/person with the remaining air (7.5 l/s/person) supplied by the MV. In both cases, air exited at the floor level. The detailed boundary conditions are summarized in Table 1.

Box-shaped mannequins were used to represent the 35 passengers in the case of the MV simulation. In the evaluation of the MV plus PV case, because part of the conditioned air was directed at the face, large concentration, velocity, and temperature gradients were expected to be formed surrounding the head. Therefore, a mannequin capturing the real body shape was helpful in capturing the various airflows (personalized airflow, room airflow, natural convection flow surrounding the warm body, etc.) and their interaction in the breathing zone. We have developed a numerical thermal mannequin (NTM) through laser scanning with the real geometry of a human body (Fig. 2). This NTM was put into one seat of the cabin to replace one of the box-shaped mannequins. Both mouth and nose openings were specially furnished to simulate the sneezing, coughing, and the respiratory process.

Exposure of the passenger with the detailed body geometry model to pollutants from three kinds of sources was analyzed here: the floor surface, all 34 passenger body skins (the exposed passenger was not included), and one passenger nose [the second passenger from the left in the last row; the nose coordinate is (0.85, 3.874, 1.0)]. This passenger was assumed to be the infected person. These cases are practically meaningful when we concern dust from the floor, the bioeffluent and odor of the human body, and viruses from saliva

Presented as Paper 514 at the The 45th AIAA Aerospace Science Meeting and Exhibit, Reno, Nevada, 8–11 January 2007; received 5 February 2007; revision received 12 July 2007; accepted for publication 14 July 2007.

*Department of Building Services Engineering; bejlniu@polyu.edu.hk.

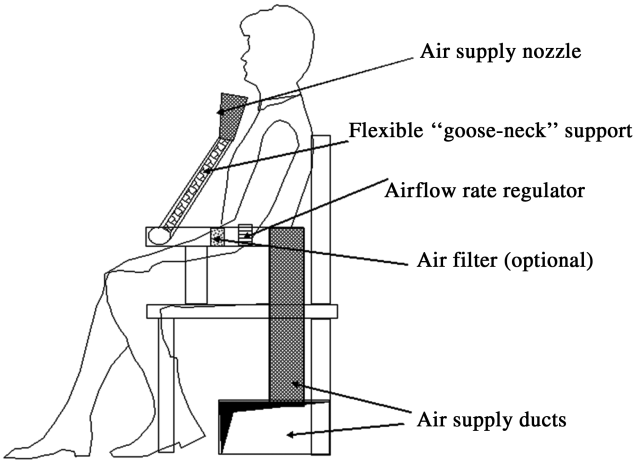

Fig. 1 A ventilation seat with an adjustable personalized air supply nozzle.

droplets produced during talking. Steady inhalation through nose at a flow rate of 0.14 l/s is assumed for the exposed passenger.

Particle-involved sneezed airflow is simulated by both a simplified Eulerian method, that is, a drift-flux model, and the Lagrangian method. The temporal evolution of particle concentrations in the cabin air can be captured by the Eulerian treatment, whereas the Lagrangian modeling can provide the trajectory of each particle. The particles are assumed to be spherical with a diameter of 1.0 μm and a material density of 1000 kg/m^3. In both methods, one-way coupling was adopted due to the fact that it was a dilute two-phase flow and the modification of particles on turbulence could be ignored. In the drift-flux model, the sneezed air released horizontally from the mouth lasted 0.5 s at a temperature of 31°C; and a velocity of 20 m/s (in the negative y direction). In a real situation, the sneezed airflow orientation may vary. A form of horizontal advance contained the highest momentum in the fore and aft directions. The spatial particle concentration was normalized by the concentration at the mouth. The governing equation of the particle concentration was similar to the gaseous pollutant equation, except that it integrated the gravitational settling effect of particles into the convection term:

$$\frac{\partial(\rho C)}{\partial t} + \nabla\cdot(\rho(\boldsymbol{U}+\boldsymbol{V}_S)C) = \nabla\cdot\left(\frac{\mu_{\text{eff}}}{\sigma_C}\nabla C\right) + S_C \qquad (1)$$

Because a net transport of particles toward solid surfaces creates concentration gradients, particle deposition was taken into account at the walls with the help of a semi-empirical deposition model [5].

In the Lagrangian method, the trajectory of a discrete phase particle was predicted by integrating the force balance on the particle. The momentum equation was expressed as:

$$\frac{\mathrm{d}\boldsymbol{u}_p}{\mathrm{d}t} = \boldsymbol{F}_{\text{drag}} + \boldsymbol{F}_{\text{grav}} + \boldsymbol{F}_{\text{addi}} \qquad (2)$$

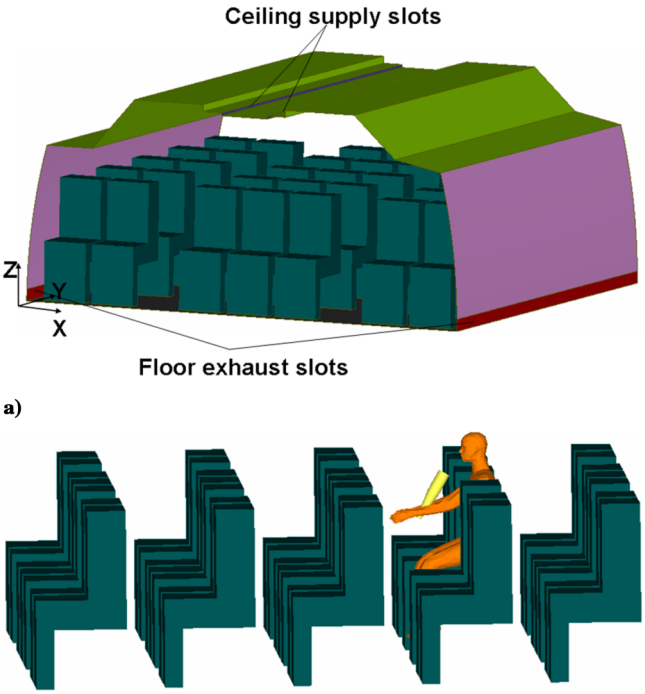

Fig. 2 Schematic of the mixing air distribution systems in a five-row section of a Boeing 767-300.

$\boldsymbol{F}_{\text{drag}}$ and $\boldsymbol{F}_{\text{grav}}$ can be written as

$$\frac{18\mu}{\rho_p d_p^2 C_C}(\boldsymbol{U}-\boldsymbol{u}_p)$$

and $\frac{\boldsymbol{g}(\rho_p-\rho)}{\rho_p}$, respectively, for which the Cunningham correction to Stokes' drag law was computed from

$$1+\frac{2\lambda}{d_p}(1.257+0.4e^{-(1.1d_p/2\lambda)})$$

The third term in Eq. (2) represents the additional forces exerted on the particles. In the current study, the thermophoretic force, Brownian force, and Staffman's lift force were taken into account. The effect of turbulence on particle dispersion was determined using a stochastic method, that is, the discrete random walk model to simulate the fluctuating velocity. The calculation on particle trajectories is terminated if the particle meets solid surfaces and the particle is considered to be trapped by them.

The numerous rows of seats were represented by using a periodic boundary condition along the Y direction. The renormalization group k–ε model including buoyancy force effect was employed to simulate the nonisothermal, time-averaged turbulent airflow fields.

Table 1 Boundary conditions

Item	Mixing ventilation	Mixing ventilation and personalized ventilation	
		MV	PV
Supply air rate, l/s/person	10	7.5	2.5
Supply air velocity, m/s)	1.35	1.34	0.5
Supply air temperature, °C	19	19	24
Ceiling temperature, °C	22	22	22
Sidewall temperature, °C	21	21	21
Floor temperature, °C	22	22	22
Human body temperature, °C	31	31	31

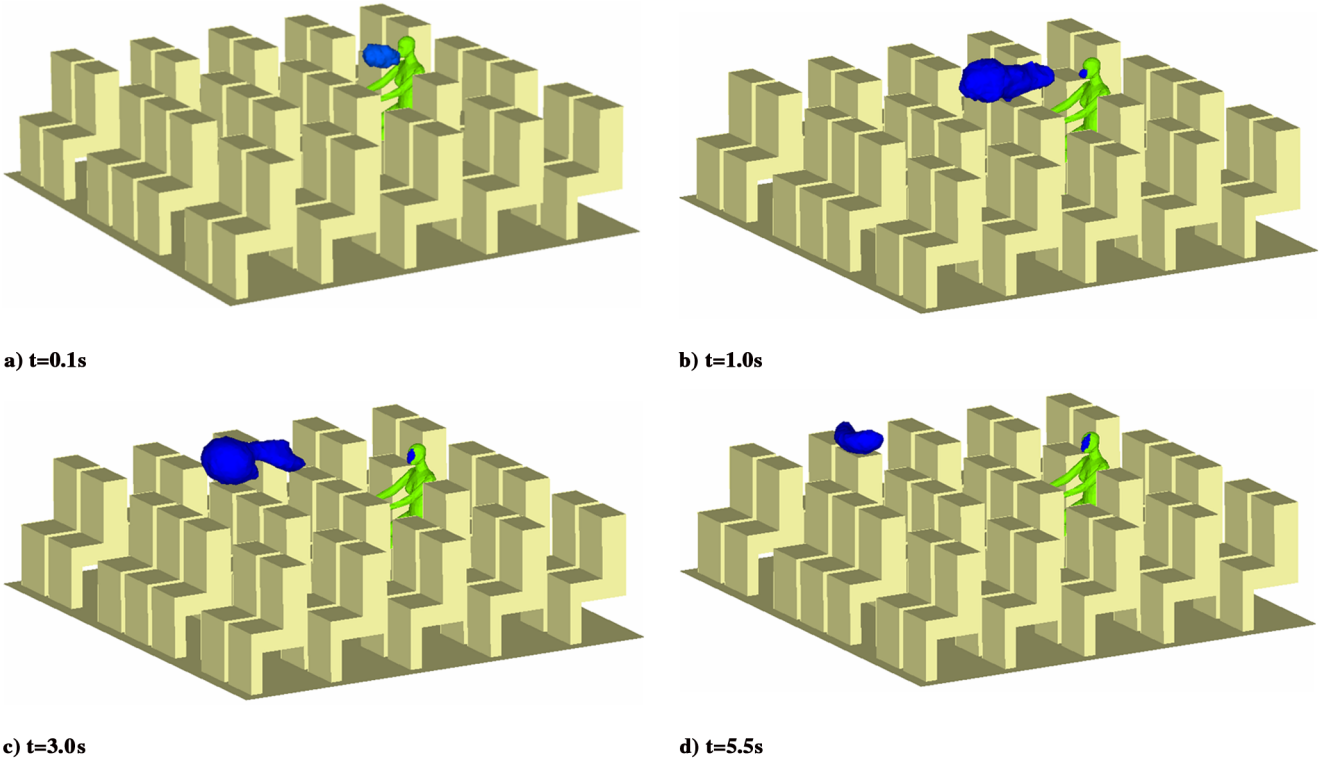

Fig. 3 Three-dimensional views of particle concentrations at various times after sneezing (the cloud shown has particle concentrations above 0.01, obtained using the Eulerian method).

III. Results and Discussions

A. Transient Dispersion of Human-Generated Aerosols

Figure 3 shows three-dimensional views of the evolution of the particle concentrations after sneezing using the Eulerian method. The blue color denotes the region where the concentration is higher than 1%. Because of the high horizontal momentum, the sneezed air was impelled to the front. The airflow also ascended slightly because the density of the warm sneezed air was less than the density of the ambient air. This pulse airflow lost its momentum quickly, accompanied by an intensive attenuation of air velocity. The particles in the sneezed air were diluted into the cabin air along their dispersion path over the seat rows. Their concentration was still higher than 1% even when the sneezed air reached the frontal three seat rows at $t = 5.5$ s. This phenomenon highlights the possibility of the airborne transmission of viruses via the sneezed/coughed droplets.

The two main transmission routes for respiratory infections are by large droplets spread over short distances and by the smaller droplets carried with the airstream over the airborne route. The airborne transmission route means the inhalation of droplets of saliva released into the air by an infected person from coughing or sneezing; these droplets (usually less than 10 μ) can remain suspended in the air for a considerable time. Large droplets will settle out of the airstream quickly and deposit on solid surfaces. Direct contact of large droplets generated from coughing, sneezing, or talking onto the mucous membranes of recipients requires contact at a close range, which is usually within 1 m.[†] According to the U.S. Centers for Disease Control and Prevention, SARS seems to spread mainly by close person-to-person contact. Brundrett [6] concluded that the risk of cross infection is primarily determined by the exposure time in the vicinity of the index passenger and that the chances of infection are very low on most flights. On one flight carrying one symptomatic patient, 22 passengers were infected, among whom 90% were seated more than 1 m away from the index patient. Therefore, airborne small particle transmission may be a more straightforward explanation [7]. In the largest in-flight SARS outbreak, on a Boeing 737-300 aircraft traveling from Hong Kong to Beijing on 15 March 2003, the passengers seated 7 rows in front and 5 rows behind the infected passenger were affected [1]. In a tuberculosis infection case on commercial flights in 1994, Kenyon et al. [8] found that passengers seated within two rows of the index patient were more likely to have positive tuberculin skin tests than those in the rest of the section. Based on these facts, we may conclude that the transport of human-generated viruses in the longitudinal direction is possible, and has a great probability of happening in the vicinity of the index passenger. Current simulation results agree well with this conclusion.

Figure 4 shows the individual particles' locations, which were obtained by the Lagrangian method. Here, to reduce computing demands, the transient sneezed airflow field was simplified as a continuous jet flow from the mouth at a speed of 20 m/s. It should be noted that this assumption would overestimate the horizontal throw of the sneezed airflow, leading to a more serious situation of virus transmission than would occur in actual cases. Particles were released from the mouth every 0.025 s in the time slot from 0 to 0.5 s. At each time step (every 0.025 s), 20 particles were generated and a total of 400 particles were tracked in one sneezing process. The particle dispersion characteristic was in line with the result from the Eulerian method except that the dispersion was much faster. At $t = 5.5$ s, most particles reached the fifth seat row in front of the sneezing passenger. To obtain statistically stable results, 400 particles were not enough. Table 2 lists the particles' final fate by tracking 1600, 4800, and 9600 particles. For each particle number, 10 occurrences of tracking are performed and the averages are shown in Table 2. It seemed that the discrepancy between 4800 and 9600 particles was negligible, indicating that 9600 particles were statistically enough. More than one third of the sneezed particles deposited onto the other passengers' body surfaces, and less than one fifth of the particles were exhausted out of the cabin. For coarse particles (20.0 μm), the portion of particles that deposited onto the inner-cabin surfaces and human bodies increased, and only about 18% of the particles were ventilated out. The high percentage of deposition in the cabin environment may be attributed to the high surface-to-volume ratio. This challenges previous ideas that the use

[†]Data available online. See J. S. Garner's "Guideline for Isolation Precautions in Hospitals," Atlanta: Centers for Disease Control and Prevention, http://www.cdc.gov/ncidod/dhqp/gl_isolation.html [retrieved 22 June 2007].

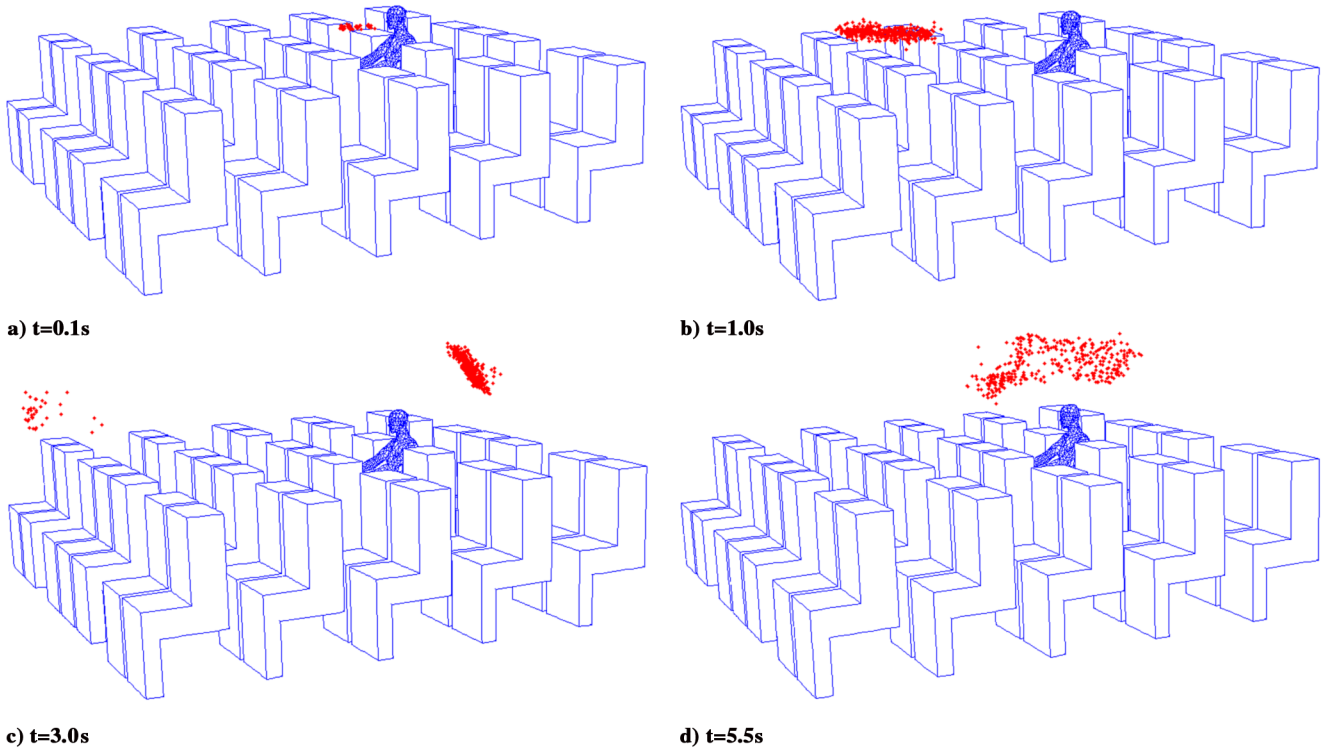

Fig. 4 Three-dimensional views of temporal particle dispersion after sneezing (obtained using the Lagrangian method).

of high-efficiency particulate arrestance-type filters in aircraft cabin pressurization systems can ensure that 99.9% of bacteria and viruses produced by aircraft passengers are removed from cabin air, and may imply that surface disinfection is required for more effective infection control.

B. Human Exposure and Personalized Ventilation

The ventilation efficiency of the PV was closely related to the local airflow field in the breathing zone. Figure 5 shows the flow path lines of personalized air. The cool and fresh personalized air was directed at the face, guaranteeing fresh inhalation air and the elimination of stuffy sensations. Given a tracer gas concentration of 1000 ppm in the personalized supply nozzle, the inhaled tracer gas concentration was 586 ppm. Therefore, 58.6% of inhaled air came from the clean personalized air. In other words, 58.6% of the contaminants in the ambient cabin air can be shielded by this type of PV. One may question the sensitivity of the personalized ventilation efficiency with regard to a correct positioning of air supply nozzle. This problem commonly appears in most types of PV systems because the PV, a form of microventilation, requires the breathing zone in the "target area." A solution for this problem is manually adjusting the nozzle or automatically detecting the body posture [9]. In Table 3, a comparison of mixing ventilation and mixing ventilation plus personalized ventilation performance is given. Under the existing air distribution design, the inhaled pollutant concentration was even higher than the perfect mixing value, that is, 1.0, when the pollutant was produced from the floor or body surfaces, due to the spatial

Table 2 Distribution of the deposition of the sneezed particles

Particle diameter, μm	Total particles	Sneezing passenger his/herself	Other passengers' bodies, %	Cabin ceiling, %	Cabin sidewalls, %	Cabin floor, %	Inlet, %	Outlet, %
1.0	1600	0.35	33.83	28.26	9.36	8.04	0.10	20.06
1.0	4800	0.30	33.63	28.76	9.34	8.00	0.15	19.81
1.0	9600	0.31	34.04	28.13	9.51	8.10	0.15	19.76
10.0	1600	0.39	35.46	25.49	9.01	9.59	0.13	19.92
10.0	4800	0.32	35.67	25.85	8.83	9.16	0.17	20.00
10.0	9600	0.35	35.93	25.70	8.85	9.31	0.11	19.74
20.0	1600	0.36	41.88	18.96	6.79	14.03	0.06	17.92
20.0	4800	0.41	41.76	18.75	6.95	14.10	0.07	17.95
20.0	9600	0.42	41.67	18.88	6.95	14.02	0.07	17.99

Table 3 Passenger exposures

	Pollutants from floor[a]	Pollutants from bodies[a]	Pollutants from another's nose[a,b]
MV	1.26	1.33	0.81
MV + PV	0.59	0.52	0.37

[a]The exposure was normalized by the pollutants' concentration at the exhaust. It meant that exhaust concentration was 1.0.
[b]The pollutant was generated from the nose of one passenger [the second passenger from the left in the last row; the nose coordinate is (0.85, 3.874, 1.0)]. The generation rate was 0.12 g/s. The steady exposure in the MV and the MV + PV was 39.1 and 19.0 ug/s, respectively.

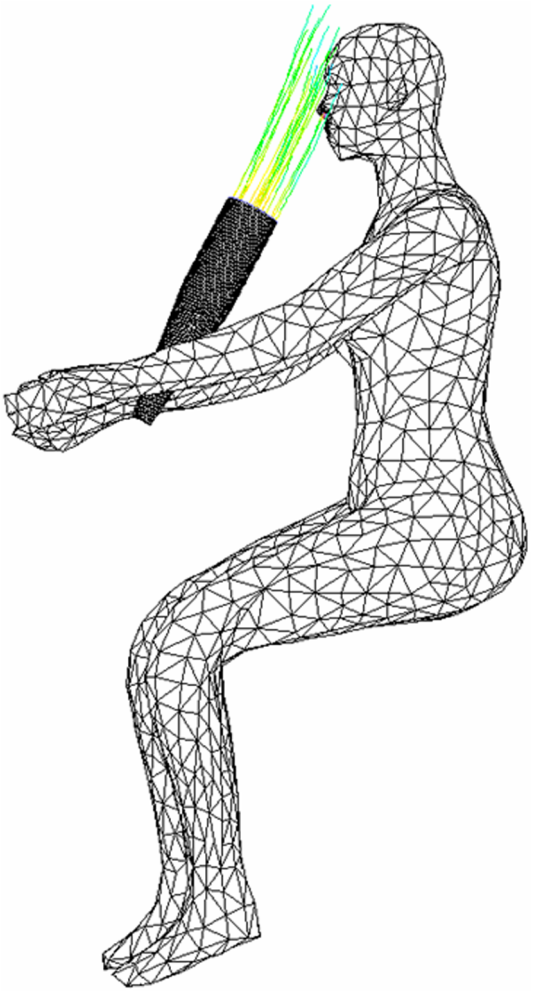

Fig. 5 Flow path lines at the facial region with personalized ventilation.

nonuniformity of pollutant distribution. Exposure to pollutants from another passenger's nose was 39.1 μg/s in the existing ventilation design and was decreased to 19.0 μg/s if the personalized ventilation functioned, when the pollutants generation rate was assumed to be 0.12 g/s. This means a PV could decrease the exposure by about 53–60% in the three cases, exhibiting an encouraging effect of personalized air supply in the aspect of airborne transmission control.

IV. Conclusions

In this study, the cabin airflow field is simulated in a five-row section of a Boeing 767-300 aircraft. Because of the high-occupancy density, the transmission of respiratory diseases could be significant due to direct contact or by airborne routes, as illustrated by both the Eulerian and Lagrangian methods. This study created a better understanding of how airborne diseases might be spread on commercial aircraft. Sneezed or coughed virus-containing particles with high momentum were able to travel a distance of more than three seat rows. Most of these particles deposit onto the passengers' bodies and inner-cabin surfaces rather than being ventilated out. This discouraging result can be offset to a certain extent by the application of personalized ventilation. This flexible, low-velocity air supply nozzle is integrated with the seat and shields up to 60% of the pollutants in the user's inhalation, potentially reducing the infection probability in commercial flights. It should be noted that this enhanced pollutant exposure reduction is achieved without increasing the total ventilation rate and, therefore, would not increase the operation cost of the cabin environmental control system.

References

[1] Mangili, A., and Gendreau, M. A., "Transmission of Infectious Diseases During Commercial Air Travel," *Lancet*, Vol. 365, No. 9463, 2005, pp. 989–994.
doi:10.1016/S0140-6736(05)71089-8

[2] Spengler, J. D., and Wilson, D. G., "Air Quality in Aircraft," *Journal of Process Mechanical Engineering*, Vol. 217, No. 4, 2003, pp. 323–335.
doi:10.1243/095440803322611688

[3] Leder, K., and Newman, D., "Respiratory Infections During Air Travel," *Internal Medicine Journal*, Vol. 35, No. 1, 2005, pp. 50–55.
doi:10.1111/j.1445-5994.2004.00696.x

[4] *Fluent 6.2 User's Guide*, Fluent, Inc., Lebanon, NH, 2005.

[5] Lai, A. C. K., and Nazaroff, W. W., "Modeling Indoor Particle Deposition from Turbulent Flow onto Smooth Surfaces," *Journal of Aerosol Science*, Vol. 31, No. 4, 2000, pp. 463–476.
doi:10.1016/S0021-8502(99)00536-4

[6] Brundrett, G., "Comfort and Health in Commercial Aircraft: A Literature Review," *Journal of the Royal Society for the Promotion of Health*, Vol. 121, No. 1, 2001, pp. 29–37.
doi:10.1177/146642400112100108

[7] Olsen, S. L., Chang, H. L., Cheung, T. Y., Tang, A. F., Fisk, T. L., Ooi, Sp., Kuo, H., Jiang, D. D., Chen, K., Lando, J., Hsu, K., Chen, T., and Dowell, S. F., "Transmission of the Severe Acute Respiratory Syndrome on Aircraft," *New England Journal of Medicine Medical Progress Series*, Vol. 349, No. 25, 2003, pp. 2416–2422.

[8] Kenyon, T. A., Valway, S. E., Ihlf, W. W., Onorato, I. M., and Castro, K. G., "Transmission of Multidrug-Resistant Mycobacterium Tuberculosis During a Long Airplane Flight," *New England Journal of Medicine Medical Progress Series*, Vol. 334, No. 15, 1996, pp. 933–938.

[9] Jacobs, P., and Gids, W. F., "Individual and Collective Climate Control in Aircraft Cabins," *International Journal of Vehicle Design*, Vol. 42, Nos. 1/2, 2006, pp. 57–66.
doi:10.1504/IJVD.2006.010177